International Journal of Mass Spectrometry 301 (2011) 224–233

Contents lists available at ScienceDirect

International Journal of Mass Spectrometry

journal homepage: www.elsevier.com/locate/ijms

# Concomitant EDD and EID of DNA evidenced by $MS^n$ and double resonance experiments

Viet Hung Nguyen, Carlos Afonso, Jean-Claude Tabet*

*Equipe de Spectrométrie de masse, Institut Parisien de Chimie Moléculaire, CNRS-UMR 7201, Université Pierre et Marie Curie-Paris6, 4 place Jussieu, Bat F, 7eme etage, Boite 45, 75252 Paris Cedex 05, France*

ARTICLE INFO

*Article history:*
Received 15 April 2010
Received in revised form 3 August 2010
Accepted 13 October 2010
Available online 20 October 2010

*Keywords:*
FT-ICR
EDD
Double resonance
DNA
Electrospray

ABSTRACT

Under collisional activation condition, it is well known that dissociations of multideprotonated oligonucleotides involve an initial loss of nucleic base (formation of $[M-nH\text{-}B_i]^{n-}$) yielding consecutively the complementary ($a_i$-B) and $w_j$ product ions. The loss of thymine is thermodynamically unfavored owing to its low proton affinity. 6 mer DNA anions were activated in SORI-CID and by EDD. The EDD spectra are significantly different from SORI-CID. All EDD spectra showed singly charged $w_5^-$ with good abundance, while this ion was not detected in SORI-CID spectra. In EDD spectra loss of thymine is easily detected, surprisingly doubly charged fragment ions were also detected, these ions can be produced directly from precursor ion $[M-2H]^{2-}$. $MS^3$ and double resonance experiments have been realized to find the origin of these doubly charged and $[a_i\text{-}T]^-$ ions in EDD spectra of $d(T_2AT_3)$ and $(T_2CT_3)$. It has been demonstrated that these doubly charged ions are produced by electron induced dissociation. The combination of double resonance and EDD/SORI-CID $MS^3$ experiments allows decoupling the EID from the EDD processes.



## 1. Introduction

Electrospray is a soft ionization method allowing to analyze high molecular mass species such as oligonucleotides [1–3]. Electrospray can preserve non-covalent interaction allowing, for instance to investigate the secondary structure of oligonucleotides [4]. Different ion activation techniques have been used and the most common is collision-induced dissociation (CID) [5,6]. However, under CID, thymine-rich DNA can yield incomplete sequence information [7,8]. In fact, it has been shown that dissociations of multideprotonated DNA involve as first step a loss of nucleic base (i.e., formation of $[M-nH\text{-}B_i]^{n-}$) yielding consecutively the ($a_i$-$B_i$) and $w_j$ complementary product ions [8–10]. The loss of thymine is thermodynamically unfavored owing to its relatively low proton affinity which explains the higher stability of thymine rich oligonucleotides [11,12].

Electron capture process (ECD) [13–15] has been developed originally by Zubarev et al. This method is carried out typically on multiprotonated molecules using low kinetic energy electrons (0–2 eV). The electron capture is exothermic (5–7 eV), due to the decrease of charge state, yielding radical driven covalent bond cleavages [16]. This dissociation mode is widely used for post-translationally modified peptides because the ECD process occurs along the peptide backbone [16,17]. Complementary to ECD, EDD (electron detachment dissociation) is dedicated to multideprotonated molecules. The negative ion mode is chosen due to the presence of several phosphate groups considered as strong acidic sites in the gas phase. Generally, EDD takes place with higher kinetic energy electrons (>10 eV) [18–20]. The electron motion is related to a frequency whose wavelength depends on the kinetic energy causing the detachment of one or several electrons (electron stripping) [21,22]. Xu et al. investigated double-stranded oligonucleotides associated with drug by EDD [20]. They observed very good electron detachment efficiency without significant fragmentations. Hakanson and co-workers investigated short single-stranded oligonucleotides (i.e., 6 mer) by EDD and they observed some fragment ions which differ from those observed with ergodic activation methods such as CID or IRMPD [23]. Recently, using double resonance to eject $a^\bullet/z^\bullet$ odd-electron ion during the EDD experiments, it was found that the abundance of the $[a/z\text{-}T]^-$ ion decreased [24]. This result suggested that the formation of the $[a/z\text{-}T]^-$ ions is produced through the consecutive dissociation of the odd-electron $a^\bullet/z^\bullet$ ions.

Different activation methods can be used for electron stripping from multiply charged negative ions. For instance, this process can take place by electron photodetachment dissociation (EPD) under UV irradiation conditions [25,26]. Using this method Gabelica et al. [25] showed that electron detachment is nucleobase dependent (presence of guanine). However, very few fragment ions have been observed in EPD. It should be noted that under high-energy collision condition [27,28] (several keV), electron detachment process (or electron stripping) can be observed.

* Corresponding author. Tel.: +33 1 44 27 32 64; fax: +33 1 44 27 38 43.
*E-mail address:* jean-claude.tabet@upmc.fr (J.-C. Tabet).

1387-3806/$ – see front matter © 2010 Elsevier B.V. All rights reserved.
doi:10.1016/j.ijms.2010.10.018

The aim of this study was to compare the fragmentation patterns of multideprotonated DNA under SORI-CID and EDD conditions. Especially, sequential $MS^3$ and double resonance experiments were performed on the charge reduced odd-electron anion, in order to acquire additional details on the EDD mechanisms. By this way the contribution of EDD and EID in the spectra could be demonstrated. The behavior of deprotonated DNA and the influence of nucleobases toward EDD processes were scrutinized. Finally some mechanisms were proposed to explain the fragmentations involving radical promoted processes.

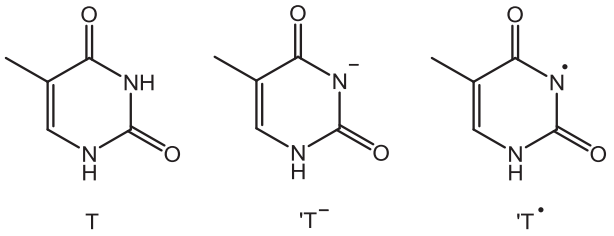


**Scheme 1.** Nomenclature used for nucleobase losses (case of thymine).

## 2. Experimental

### 2.1. Sample preparation

All DNA were obtained from EUROFINS MWG Biotech (Ebersberg, Germany) and used without further purification. All other chemicals have been purchased from Sigma–Aldrich Chemicals (St Quentin Fallavier, France). Samples have been prepared using deionized water (18.2 MΩ) and HPLC grade methanol 80/20 with 2 mM ammonium acetate. The final concentration of DNA solutions was 20 μM.

### 2.2. Mass spectrometry

All experiments were conducted on an actively shielded 7 T hybrid quadrupole Fourier transform ion cyclotron resonance (Qh-FT/ICR) mass spectrometer (ApexQe, Bruker Daltonics, Billerica, USA). The DNA solutions were infused in an Apollo II electrospray ion source at a flow rate of 120 μL $h^{-1}$ with the assistance of $N_2$ nebulizing gas. Ionization was performed in negative mode with an ESI voltage of 3500 V. The capillary exit was set to 300 V; skimmer I was set 40 V; and skimmer II was set to 8 V. All ESI mass spectra were acquired with XMASS (version 6.1, Bruker Daltonics) in broadband mode from *m/z* 200 to *m/z* 2000. The image signal was amplified and digitized using 512 K data point resulting in the recording of a 0.47 s time domain signal which was transformed into the corresponding frequency domain by Fourier transform (one zero fill and Sinbell apodization).

For EDD experiments, higher kinetic energy electrons have been produced from an indirectly heated hollow dispenser cathode (inner and outer diameters of 3.5 mm and 7.6 mm, respectively, located 88 mm from the ICR cell) and were introduced into the ICR cell for 3 s. A heating current of 1.5 A was applied to a heater element located behind the cathode, and the bias voltage was 19.5 V. A lens electrode (6 mm inner diameter) located immediately in front of the cathode was kept at −20 V. Sustained Off-Resonance Irradiation Collision-Induced Dissociation (SORI-CID) was accomplished using Argon as collision gas. The ions were excited using an excitation amplitude of 3.4 $V_{p,p}$ with a frequency offset of 600 Hz applied for 250 ms. A pumping delay of 2 s was used before the excitation/detection step.

All mass spectra have been internally calibrated. Reported *m/z* ions were compared to the theoretical *m/z* and ions with an error more than 10 ppm were not considered.

The signals of the ESI mass spectra (and product ions spectra) have been labeled using Mcluckey's [29] nomenclature which has been modified as following. In order to describe the release of nucleic base in molecule, radical or anion forms, the nomenclature was changed using B capital (Scheme 1) instead of BH for nucleobase. Apostrophe was used to show that one H was missing (i.e., 'B). An anion or radical species, were noted as 'B⁻ or 'B•. It was demonstrated that, negative ion activation by electron bombardment was a mixture of EDD and EID (electron induced dissociation) processes. Most fragment ions originate from charge reduced ion consecutive dissociation (EDD) whereas some fragment ions were produced directly from the precursor ion without electron detachment (EID). Therefore, conventional EDD was designated here as EDD–EID.

## 3. Results

### 3.1. SORI-CID spectra of 6 mer DNA

Several 6 mer DNA (i.e., $d(GT_5)$, $d(G_3T_3)$, $d(T_2AT_3)$, $d(T_2CT_3)$, $dT_6$ and d(GCATGC)) containing variable thymine number were investigated under SORI-CID conditions. Low excitation amplitude was chosen (3.4 V) to avoid extensive consecutive decompositions. Doubly deprotonated DNA were the most abundant ions in the ESI mass spectra (data not reported). These doubly charged ions were selected and activated under SORI-CID conditions. The product ion spectrum of $[d(GT_5)\text{-}2H]^{2-}$ (*m/z* 892) (Fig. 1a) displayed the $w_5^{2-}$ ion (*m/z* 768) without formation of the corresponding singly charged $w_5^-$ ion (*m/z* 1537). Complete $w_j^-$ ion series is detected but most ions are produced with a very low abundance except $w_5^{2-}$. Note that the direct G release ($[M-2H-G]^{2-}$, *m/z* 817) is observed whereas no loss of thymine is detected. The $w_5^{2-}$ ion is observed which carries the entire initial charge of the precursor ion so $[a_1\text{-}G]^-$ ion (*m/z* 115) cannot be detected. The SORI-CID spectrum of the $[d(G_3T_3)\text{-}2H]^{2-}$ ion (*m/z* 917) (Fig. 1b) showed only complementary product $w_j/(a_i\text{-}B)$ ions (with $j = 3,4$ and $i + j = 6$) corresponding to the cleavages in the guanine-rich region. Again, the $[a_1\text{-}G]^-$ ion (*m/z* 115) is not observed since $w_5^{2-}$ is still present. Nevertheless, the $w_5^{2-}$ ion abundance decreases while those of $w_4^{2-}$ and $w_4^-$ are reinforced. The direct G loss is favored and thus, the internal fragment $[G_2{:}G_2]^-$ (*m/z* 506) ion appeared. The SORI-CID spectra of $[M-2H]^{2-}$ ions (*m/z* 884) of $d(T_2AT_3)$ (Fig. 1c) and $d(T_2CT_3)$ (*m/z* 872) (Fig. 1d) display respectively direct losses of A and C. However, the complementary $[a_3\text{-}B]^-/w_3^-$ ions (*m/z* 705 and *m/z* 929, respectively) emerge with similar abundances. Note that the relative abundance of the $[a_3\text{-}A]^-$ ion (*m/z* 705) is significantly higher than that of the $[a_3\text{-}C]^-$ ion (*m/z* 705). In the same way the $[M-2H-A]^{2-}$ ion (*m/z* 817) is significantly more abundant than the $[M-2H-C]^{2-}$ ion (*m/z* 817). Finally, among the low-abundant product ions, the complete $w_j^-$ series is detected either as singly charged ($w_1^-$, $w_2^-$ and $w_3^-$) or as doubly charged ($w_4^{2-}$ and $w_5^{2-}$) ions. It should be noted that the singly charged $w_4^-$ and $w_5^-$ ions were not detected. The SORI-CID spectrum of the $[dT_6\text{-}2H]^{2-}$ ion (*m/z* 880) (Fig. 1e) also displays the complete $w_j$ ion series. In addition, ion series involving thymine base release ($[a_i\text{-}T]^-$, $i = 2$–5) were detected in very low abundance. This illustrates the difficult thymine base loss, although it can occur through a low rate constant reaction. Finally, the SORI-CID spectrum of $[M-2H]^{2-}$ (*m/z* 894) of d(GCATGC) (Fig. 1f) that presents only one thymine base is more informative. This spectrum displayed, in particular, more internal fragment ions (i.e., $[C_2{:}C_2]^-$, $[T_4{:}T_4]^-$, $[A_3{:}T_4]^-$ and $[C_2{:}T_4]^-$ at *m/z*, 446 *m/z* 481, *m/z* 794 and *m/z* 1083, respectively) than those occurring from the other investigated DNA. In addition, the $w_1^-$ (*m/z* 306) ion abundance was strongly enhanced and the direct competi-

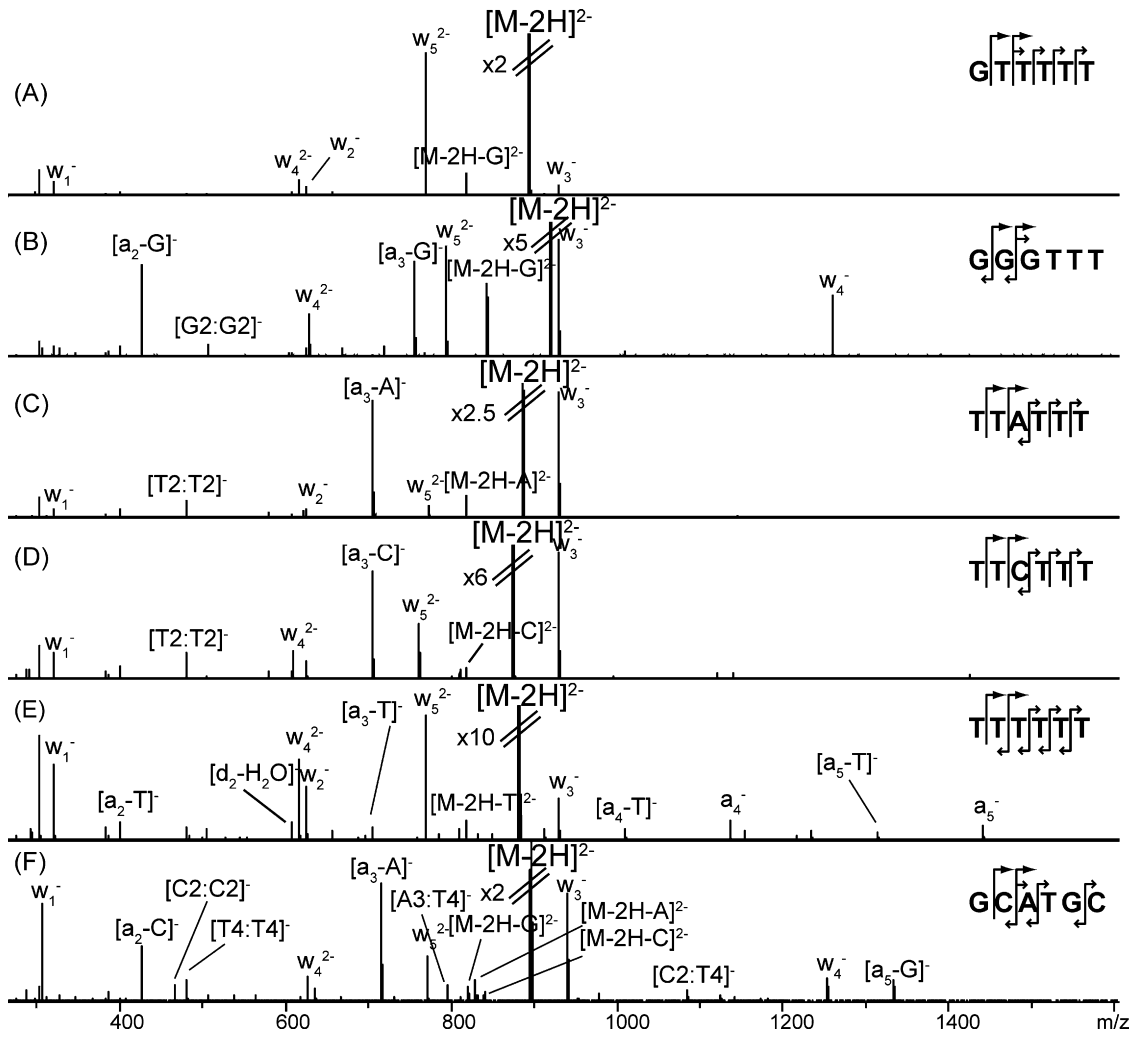


**Fig. 1.** SORI-CID spectra of 6 mer DNA $[M-2H]^{2-}$ ions. (a) d($GT_5$) ($m/z$ 892), (b) d($G_3T_3$) ($m/z$ 917), (c) d($T_2AT_3$) ($m/z$ 884), (d) d($T_2CT_3$) ($m/z$ 872), (e) $dT_6$ ($m/z$ 880) and (f) d(GCATGC) ($m/z$ 894). The open arrow denotes singly charged ions and closed arrow the doubly charged ions.

tive losses of guanine, adenine and cytosine yielded the $[M-2H-B]^-$ ($m/z$ 1639 $m/z$ 1655 $m/z$ 1679 respectively) series. The almost complete $[a_i\text{-}B_i]^-$ ion series is detected (except for $i=1$ and 4).

All collisionally activated 6 mer oligonucleotides produced singly charged $w_j^-$ ions (with $j<5$) depending on the nucleotide sequence and more particularly of the nucleobase proton affinity. Complementary ions were observed for $j=3$ as $[a_3\text{-}B]^-$ (with $B \neq T$). The singly charged $w_5^-$ was never observed but the $w_4^-$ ion is produced competitively with the $w_4^{2-}$ ion. In the case of a more random nucleotide sequence (i.e., d(GCATGC)) presenting only one thymine, the entire $[a_i\text{-}B]^-/w_{6-i}^-$ series was detected (except for $i=1$, 4 due to the presence of $w_5^{2-}$ and thymine, respectively).

### 3.2. EDD–EID spectra of 6 mer DNA d($T_2AT_3$) and d($T_2CT_3$)

Fig. 2a shows the EDD–EID spectrum of doubly deprotonated d($T_2AT_3$) ($m/z$ 872) (the product ion assignments are given in Table 1). This spectrum displayed a complete series of singly charged $w_j^-$ ions allowing a simple sequence determination. It is noteworthy that the relative abundance ratio between $w_3^-$ ($m/z$ 929) and $w_5^{2-}$ ($m/z$ 760) in the EDD–EID spectrum are similar to that displayed in the SORI-CID spectrum (Fig. 1c). Furthermore, the $w_4^-$ ($m/z$ 1218) and $w_5^-$ ($m/z$ 1522) singly charged ions which were absent in the SORI-CID spectrum, appeared in the EDD–EID spectrum and the abundances of $w_j^-$ ion series increased with the size of the product ions except for $w_3^-$ which is enhanced due to the location of adenine. The charge reduced $[M-2H]^{\bullet-}$ ($m/z$ 1745) ion produced through electron stripping was also detected. The low abundance odd-electron ions were very likely obtained by the consecutive decompositions of the $[M-2H]^{\bullet-}$ ion. The attribution of these signals are ambiguous, since they can correspond to the $z_j^{\bullet-}$ or $a_i^{\bullet-}$ ion series. In addition two additional product ions related to the unexpected loss of thymine (i.e., $[a_4\text{-}T]^-$ ($m/z$ 994) and $[a_5\text{-}T]^-$ ($m/z$ 1298) (or $[z_5\text{-}T]^-$) have been detected. The latter ions as well as $w_4^-$ and $w_5^-$ ions can probably be produced from dissociation of odd-electron anion, because they were not displayed in the SORI-CID spectrum (Fig. 1c). These product ions could be specific to the EDD mode. Electron bombardment of the doubly deprotonated d($T_2CT_3$) (Fig. 2b) yielded fragment ions similar to those observed for d($T_2AT_3$). In addition, $[z_n\text{-}T]^-/[a_n\text{-}T]^-$ product ions involving thymine base loss are again detected. The abundance ratio between the $w_3^-$ and $w_5^{2-}$ ions is similar to that observed in the SORI-CID spectrum of $[M-2H]^{2-}$ ion for d($T_2CT_3$) (Fig. 1d). In addition, the relative abundance of the $[a_3\text{-}C]^-$ ion ($m/z$ 705) and of its complementary $w_3^-$ ion ($m/z$ 929) is lower than that of the $[a_3\text{-}A]^-$ and $w_3^-$ ($m/z$ 929) ions displayed in the EDD–EID spectrum of d($T_2AT_3$) (Fig. 2a and b).

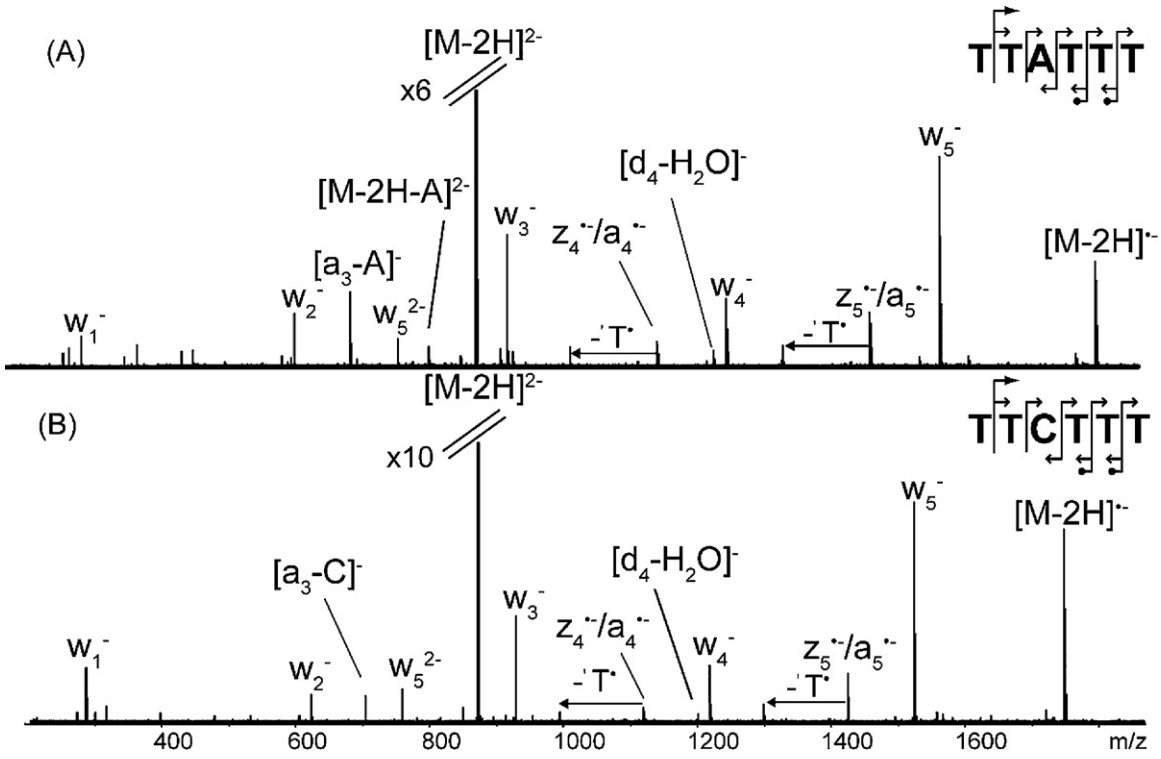


**Fig. 2.** EDD spectra of $[M-2H]^{2-}$ (a) *m/z* 884 for d($T_2AT_3$) and (b) *m/z* 872 for d($T_2CT_3$) DNA. The arrow with a dot denotes a• radical ion.

In principle, the $w_3^-$ fragment ions as well as the $w_4^-$ and $w_5^-$ ions must be produced from the consecutive decompositions of the $[M-2H](^-$ odd-electron anion. However, another decomposition pathway must be considered to explain the formation of the doubly charged $w_5^{2-}$ ion. It should be pointed out that all ions formed in the source have been ejected through a double isolation step of the precursor ion, on the quadrupole and in the ICR cell. So, the doubly charged ($[M-2H-B]^{2-}$ and $w_5^{2-}$) product ions are formed during the electron bombardment step. Therefore, they are probably produced directly from the selected precursor ion by EID [30] or from other processes.

### 3.3. Sequential $MS^3$ and double resonance experiments

In order to acquire more information on the various processes involved in EDD–EID mode and to elucidate the origin of doubly charged product ions, double resonance experiments were realized. In this case, the odd-electron $[M-2H]^{\bullet-}$ anion is continuously ejected using resonant excitation during the EDD–EID experiments. With a sufficiently high excitation amplitude, the $[M-2H]^{\bullet-}$ ions can be ejected from ICR cell before its consecutive dissociations. Consequently, only fragment ions generated from the direct decomposition of the doubly charged $[M-2H]^{2-}$ precursor can be detected. However, if the charge reduced $[M-2H]^{\bullet-}$ anion dissociates with very high rate constants, its fragment ions can be produced before complete ejection. Hence these fragment ions can be observed.

**Table 1**
Product ions observed following EDD–EID of $[T_2AT_3\text{-}]^{2-}$.

| Attribution | Theoretical (*m/z*) | Observed (*m/z*) | Error (ppm) |
|---|---|---|---|
| $w_1^-$ | 321.04878 | 321.04776 | −3.2 |
| $w_2^-$ | 625.09482 | 625.09290 | −3.1 |
| $w_5^{2-}$ | 772.61888 | 772.61622 | −3.4 |
| $[a_3\text{-}AH_3]^-$ | 705.12158 | 705.11938 | −3.1 |
| $[M-2H\text{-}AH]^{2-}$ | 817.13148 | 817.12847 | −3.7 |
| $[M-2H]^{2-}$ | 884.65873 | 884.65592 | −3.2 |
| $w_3^-$ | 929.14086 | 929.13927 | −1.7 |
| $[a_4\text{-}T_4]^-$ | 1018.17918 | 1018.17725 | −1.9 |
| $z_4^{\bullet-}/a_4^{-\bullet}$ | 1143.21428 | 1143.21287 | −1.2 |
| $[d_4\text{-}H_2O]^-$ | 1224.18612 | 1224.18591 | −0.2 |
| $w_4^-$ | 1242.19848 | 1242.19766 | −0.7 |
| $[a_5\text{-}T_5]^-$ | 1322.22522 | 1322.22653 | 1.0 |
| $z_5^{\bullet-}/a_5^{\bullet-}$ | 1447.25977 | 1447.26154 | 1.2 |
| $w_5^-$ | 1546.23723 | 1546.24072 | 2.3 |
| $[M-2H]^{\bullet-}$ | 1769.31692 | 1769.31392 | −1.7 |

Double resonance experiment was used for lifetime study of intermediate fragment ions, [31–34] and has been applied to investigate peptide dissociation by ECD [35]. Moreover, this approach that can give an idea on the origin of fragment ions, is very useful to study the dissociation mechanism and for other applications [33,36–40]. Recently Hakansson and co-workers used this approach for studying the dissociation mechanisms of deprotonated oligonucleotides [24].

Fig. 3a and c displays the double resonance spectra of $[M-2H]^{\bullet-}$ generated by electron stripping of $[M-2H]^{2-}$ for d($T_2AT_3$) and d($T_2CT_3$). The resulting profiles present fragment ions similar to those observed in SORI-CID spectra (Fig. 1c and d), except the additional $w_4^-$ ions that was not formed under CID from both the doubly deprotonated d($T_2AT_3$) and d($T_2CT_3$).

The presence of the $w_4^-$ ion, may be due to a fast decomposition of $[M-2H]^{\bullet-}$ that is therefore produced prior to its ejection. The doubly charged $[M-2H\text{-}B]^{2-}$ and $w_5^{2-}$ product ions displayed in the EDD–EID spectra (Fig. 2a and b) were maintained whereas the $a_4^{\bullet-}/z_4^{\bullet-}$ and $a_5^{\bullet-}/z_5^{\bullet-}$ product ions as well as the $[a_4\text{-}T]^-$ and $[a_5\text{-}T]^-/[z_5\text{-}T]^-$ ions disappeared in the double resonance spectra. This means that their respective formation rate constant is sufficiently low to be not produced before ejection of the charge reduced ion. In fact, the formation of these product ions take place after ejection of the $[M-2H]^{\bullet-}$ intermediate ion.

Sequential $MS^3$ experiments can give additional information on these fragment ions. The odd-electron $[M-2H]^{\bullet-}$ anions produced by electron stripping from the selected $[M-2H]^{2-}$ ions,

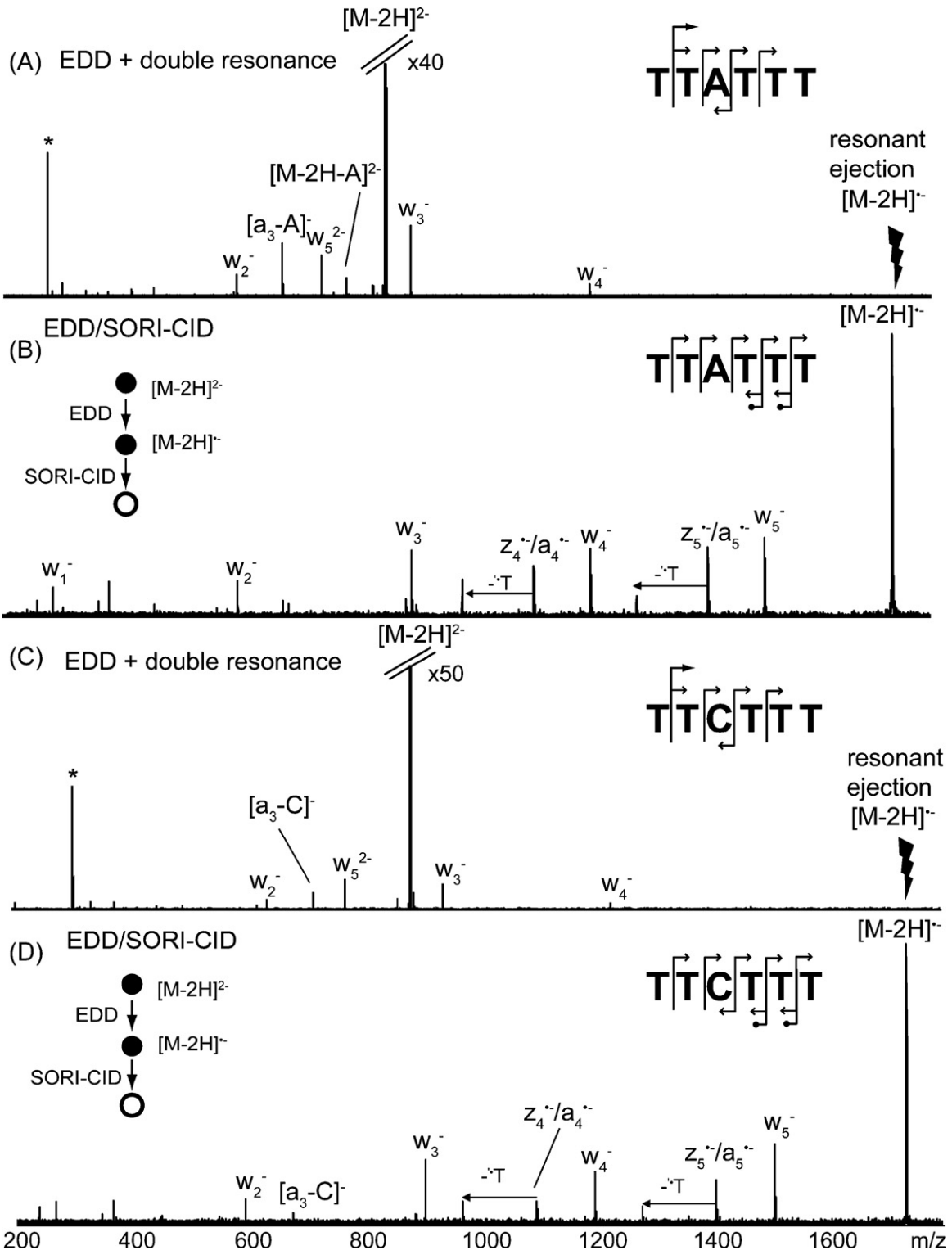


**Fig. 3.** Double resonance spectra (19 V as ejection energy) of odd-electron $[M-2H]^{\bullet-}$ prepared by EDD processes from (a) $d(T_2AT_3)$ $m/z$ 894 and (b) $d(T_2CT_3)$ at $m/z$ 872 and sequential $MS^3$ experiment by consecutive EDD (electron stripping yielding $[M-2H]^{\bullet-}$) and SORI-CID.

were activated by SORI-CID (Fig. 3b and d). The majority of the singly charged product ions detected in EDD–EID/SORI-CID spectra of $[M-2H]^{\bullet-}$ was present in the EDD–EID spectra of both the $[d(T_2AT_3)\text{-}2H]^{2-}$ and the $[d(T_2CT_3)\text{-}2H]^{2-}$ precursor ions (Fig. 2a and b). However, the $[a_3\text{-}A]^-$ ($m/z$ 705) ion for the $d(T_2AT_3)$ sequence is absent, although the corresponding $[a_3\text{-}C]^-$ ($m/z$ 705) product ion of $d(T_2CT_3)$ is detected in low abundance. It should be noted that the relative abundance of the $w_j^-$ ions are significantly reduced, with respect to the odd-electron $a_n^{\bullet-}/z_n^{\bullet-}$ ions. Interestingly, the $w_j^-$ fragment ion abundance increases with the product ion size. Finally, as expected doubly charged product ions disappeared from the sequential EDD–EID/SORI-CID spectra. These sequential $MS^3$ experiments suggested that the $[a_n\text{-}T]^-/[z_n\text{-}T]^-$ ions are most likely produced through a radical driven dissociation

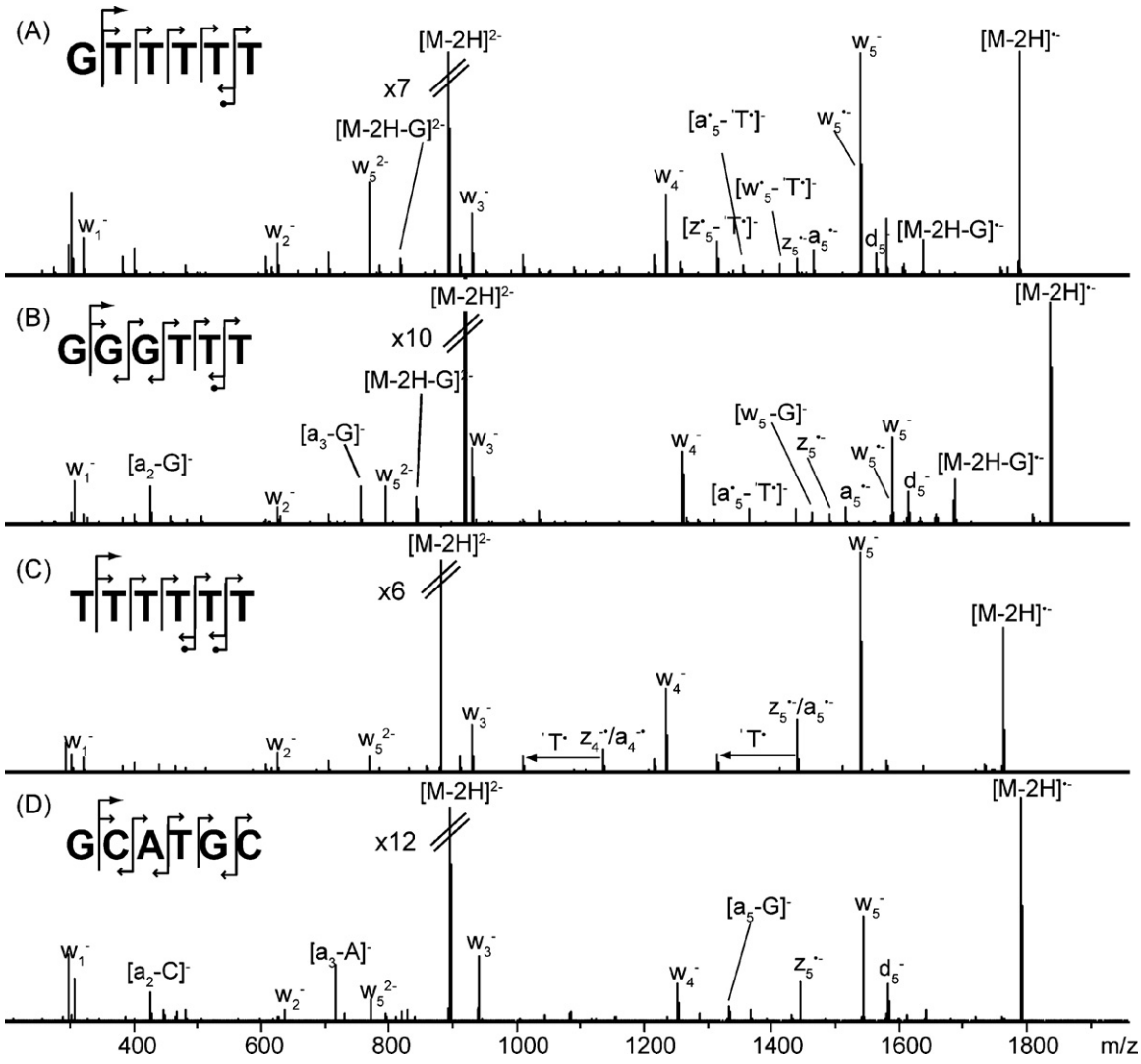


**Fig. 4.** EDD spectra of DNA (a) d($GT_5$) *m/z* 892, (b) d($G_3T_3$) (*m/z* 917), (c) $dT_6$ (*m/z* 880) and (d) d(GCATGC) (*m/z* 894).

and not directly from the $[M-2H]^{2-}$ precursor ion (charge driven pathway). Actually, the radical $a_n^{\bullet}/z_n^{\bullet}$ ions lose a radical thymine to give $[a_n^{\bullet}/z_n^{\bullet}\text{-}'T^{\bullet}]^-$ (equivalent to $[a_n/z_n\text{-}T]^-$).

### 3.4. EDD–EID spectra of other 6 mer DNA

Thymine rich DNA in association with peptides was successfully studied by our group [41], in this work, we want to extend our knowledge about these DNA sequence. Since the EDD–EID spectra of d($T_2AT_3$) and d($T_2CT_3$) produced similar fragment ions, we performed EDD–EID experiments with the d($GT_5$) and d($G_3T_3$). These DNA sequences were chosen because of the presence of one and three guanines which were expected to enhance the efficiency of EDD. The $dT_6$ and d(GCATGC) were also chosen in order to compare our experiment with previous results which were investigated by Hakansson and co-workers [23].

In contrast to the previous examples (Fig. 2a and b) the odd-electron $a_5^{\bullet-}$ and $z_5^{\bullet-}$ ions as well as the even-electron $w_j$ and $d_i$ ion series were independently detected in the EDD spectrum of $[d(GT_5)\text{-}2H]^{2-}$ (Fig. 4a). Complete $w_n$ ion series was detected while only one ion of the $d_m$ series have been detected ($d_5^-$ *m/z* 1562). In addition, the odd-electron $a_5^{\bullet-}$ (*m/z* 1463) and $z_5^{\bullet-}$ (*m/z* 1438) ions are accompanied by their satellite ions due to thymine radical loss (i.e., $[a_5\text{-}T]^-$ (*m/z* 1338) and $[z_5\text{-}T]^-$ *m/z* (1313)). The $w_5^{\bullet-}$ (*m/z* 1357) ion was observed, interestingly $[w_5\text{-}T]^-$ (*m/z* 1411) was also detected. The loss of neutral guanine takes place from both the $[M-2H]^{2-}$ (*m/z* 892) and charge reduced $[M-2H]^{\bullet-}$ precursor ion (*m/z* 1785) but no loss of guanine radical was detected.

EDD–EID spectrum of $[d(G_3T_3)\text{-}2H]^{2-}$ (Fig. 4b) displayed fragment ions similar to those detected in EDD–EID spectrum of $[d(GT_5)\text{-}2H]^{2-}$. The difference between these EDD–EID spectra is the specific presence of $[a_i\text{-}B_i]$ (i.e., $[a_2\text{-}G]^-$ *m/z* 426 and $[a_3\text{-}G]^-$ *m/z* 755) observed from $[d(G_3T_3)\text{-}2H]^{2-}$. Loss of radical guanine was detected from the odd-electron $z_5^{\bullet-}$ ion while the release of thymine radical from $z_5^{\bullet-}$ in the EDD–EID spectrum of $[d(GT_5)\text{-}2H]^{2-}$ ion was observed. From the $dT_6$ sequence, some ambiguities appeared because ions tagged $w^-$ can also be $d^-$ ions. The EDD–EID spectrum of the latter sequence (Fig. 4c) displayed the complete $w_j/d_i$ ion series. In addition the $a_4^{\bullet-}/z_4^{\bullet-}$ (*m/z* 1134) and $a_5^{\bullet-}/z_5^{\bullet-}$ (*m/z* 1438) odd-electron fragment ions were detected with satellite product ions due to thymine released. Finally in the EDD–EID spectrum of d(GCATGC) (Fig. 4d), incomplete $[a_i\text{-}B_i]^-$ ion series was observed as in its SORI-CID spectrum (Fig. 1f). Only the $z_5^{\bullet-}$ (*m/z* 1442) odd-electron species without its $[z_5\text{-}G]^-$ satellite product ion was detected. In general, all EDD–EID spectra of $[M-2H]^{2-}$ showed similar fragment ions (e.g., complete singly charged $w_n$ ion series and the presence of doubly charged $w_5^{2-}$ ions). Thymine radical can be released from both $a_i^{\bullet-}$ and $z_j^{\bullet-}$ odd-electron ions.

## 4. Discussion

The doubly charged $w_5^{2-}$ ions were detected in the SORI-CID spectra for all investigated DNA without formation of singly charged $w_5^-$ ion and its complementary ion. This behavior can be related to the initial positions of the charges that are most likely in the phosphate groups. The $[a_1\text{-B}]$ fragment ion does not present any phosphate group and is therefore expected to be lost as a neutral after dissociation of the ion–dipole complex [42,43]. The SORI-CID spectrum of $[dT_6\text{-2H}]^{2-}$ ion ($m/z$ 880) displayed $[a_i\text{-T}]^-$ ($i$ = 2–5) ion series involving a thymine base loss. This loss is difficult to rationalize through a conventional charge driven pathway. Gross et al. considered the formation of a zwitterionic intermediate produced through an intramolecular proton transfer from the 5′-phosphate simultaneously with the release of the base [7]. It was shown, by replacing phosphates with methylphosphonates in the $i$-position ($i$ = 1–4) that the abundance of $[a_{i+1}\text{-B}]^-$ decreased which is consistent with this hypothesis [9]. In contrast to the SORI-CID spectra, the EDD–EID spectrum displays the singly charged $w_5^-$ ion, this ion is probably produced through a radical driven pathway. In the SORI-CID and double resonance spectra of $[d(T_2AT_3)\text{-2H}]^{2-}$ and $[d(T_2CT_3)\text{-2H}]^{2-}$ ion, the relative abundance of $[a_3\text{-A}]^-$ ion is higher than that of $[a_3\text{-C}]^-$ ion. This behavior can be explained by the formation of zwitterions [44–46] which could be produced during the desolvation step. The protonation of dA is favored as its proton affinity is slightly higher than that of dC (dG > dA > dC > >dT [47]). Fig. 1f displayed the SORI-CID spectrum of $[d(GCATGC)\text{-2H}]^{2-}$ in which the abundance of $w_1^-$ ion ($m/z$ 306) is strongly higher than its complementary ion (i.e., $[a_5\text{-G}]^-$, $m/z$ 1332). In fact, the $w_1^-$ ion may be produced through the consecutive decomposition of many other ions whereas the $[a_5\text{-G}]^-$ ion produces consecutively internal fragment ions ($[C2{:}C2]^-$ $m/z$ 466, $[C2{:}T4]^-$ $m/z$ 1083 and $[T4{:}T4]^-$ $m/z$ 481). This hypothesis is reinforced by IRMPD experiments in which the time of activation of $[GCATGC\text{-2H}]^{2-}$ was varied (0.04 s, 0.06 s, 0.08 s and 0.1 s for each experiment, results not shown). The $[a_5\text{-G}]^-$ ion was not detected but the abundance of the $w_1^-$ ion increased significantly with the laser irradiation time, whereas the other product ion abundances decreased. This shows that $w_1^-$ has several origins, and it is reinforced through consecutive decompositions.

Our double resonance (ejection of $[T_2AT_3\text{-2H}]^{\bullet-}$ $m/z$ 1769 during EDD–EID of $[T_2AT_3\text{-2H}]^{2-}$, $m/z$ 884) (Fig. 3a) and $MS^3$ experiments (EDD–EID of $[d(T_2AT_3)\text{-2H}]^{2-}$ followed by SORI-CID of $[d(T_2AT_3)\text{-2H}]^{\bullet-}$) (Fig. 3c) showed that the $[a_3\text{-A}]^-$ ion is produced from the $[M-2H]^{2-}$ through a charge driven pathway involving most likely the formation of the $[M-2H\text{-A}]^{2-}$ intermediate ion. The doubly charged product ions were not detected in the $MS^3$ (EDD–EID/SORI-CID) spectra of odd-electron produced ions from $[d(T_2AT_3)\text{-2H}]^{2-}$ to $[d(T_2CT_3)\text{-2H}]^{2-}$ but, they were present in the double resonance spectra of these oligonucleotides (Fig. 3a and c). This result confirmed that the doubly charged product ions detected in EDD–EID spectra (Fig. 2a and b) are produced directly from the $[M-2H]^{2-}$ precursor ion by EID prior to electron detachment [48]. Actually, EID occurs when the activation energy is below energy of electron detachment but with sufficient energy to promote electronic excitation. Using this method Hadi Lioe et al. compared EID with low energy CID of singly protonated amino acids. They proposed that EID results in fragmentations involving both electronic and vibrational excitations [49]. This method was successfully applied to singly charged glycosaminoglycan saccharides [50].

Odd-electron ions ($a_4^{\bullet-}/z_4^{\bullet-}$ and $a_5^{\bullet-}/z_5^{\bullet-}$) with their satellite ions were still present in the double resonance spectra of $[d(T_2AT_3)\text{-2H}]^{2-}$ and $[d(T_2CT_3)\text{-2H}]^{2-}$ ions. These ions are not detected in the sequential $MS^3$ EDD–EID/SORI-CID spectra of $[d(T_2AT_3)\text{-2H}]^{2-}$ and $[d(T_2CT_3)\text{-2H}]^{2-}$ ions, as well as its satellite ion $[a_4^{\bullet}\text{-`T}^{\bullet}]^-$ and $[z_5^{\bullet}\text{-`T}^{\bullet}]^-$ (equivalent to $[a_4\text{-T}]^-$ and $[a_5\text{-T}]^-/[z_5\text{-T}]^-$ ions). This is consistent with the hypothesis that the $[a_4^{\bullet}\text{-`T}^{\bullet}]^-$ and $[z_5^{\bullet}\text{-`T}^{\bullet}]^-/[z_5^{\bullet}\text{-`T}^{\bullet}]^-$ are produced from the consecutive decompositions of the $a_4^{\bullet-}$ and $a_5^{\bullet-}/z_5^{\bullet-}$ ions by loss of a thymine radical (`T$^{\bullet}$).

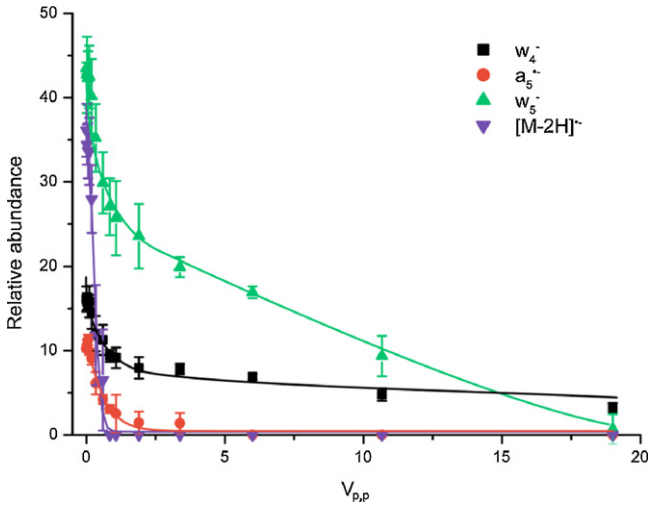


**Fig. 5.** Curves of relative abundances (abundance fragment ion 1000×/intensity of precursor ion) with variation of energy.

The singly charged $w_5^-$ ion disappeared in the double resonance spectra of the $[d(T_2AT_3)\text{-2H}]^{2-}$ and $[d(T_2CT_3)\text{-2H}]^{2-}$ ions but the $w_4^-$ ion was still observed. Nevertheless, in the SORI-CID spectra of $[d(T_2AT_3)\text{-2H}]^{2-}$ and $[d(T_2CT_3)\text{-2H}]^{2-}$ ions the $w_4^-$ ion was not detected. Our hypothesis is that the $w_4^-$ ion was produced from prompt dissociation (i.e., high dissociation rate constant). The charge reduced ion $[M-2H]^{\bullet-}$ dissociated to provide $w_4^-$ before its ejection. To confirm our hypothesis, a series of double resonance experiments of the $[d(T_2CT_3)\text{-2H}]^{2-}$ ion with various ejection amplitudes of $[d(T_2CT_3)\text{-2H}]^{\bullet-}$ ion have been realized. To our knowledge such evolution of the ion abundance as a function of double resonance amplitude was never presented for DNA. This experiment allows obtaining information on the kinetics of the different dissociation processes [51]. When the ejection amplitude was increased up to 0.75 $V_{p-p}$, the charge reduced $[M-2H]^{\bullet-}$ ion disappeared (Fig. 5) but the fragment ion abundances remained unchanged. In fact, if the time of ejection is larger than the one of the dissociation, some fragment ions can be observed in spite of ejection of the intermediate charge reduced ion. The $a_i^{\bullet-}$ radical ion series and its $[a_i^{\bullet}\text{-`T}^{\bullet}]^-$ satellite product ions disappeared from 4 $V_{p-p}$ (Fig. 5). Finally, the $w_5^-$ ion disappeared at 19 $V_{p-p}$ (Fig. 5), whereas the $w_4^-$ ion was still present. It should be noted that at 19 $V_{p-p}$, the $w_5^-$ ion was probably ejected directly by off-resonance excitation as its frequency is relatively close to that of the ejected charge reduced ion. If so, this ion can be produced through the same fragmentation pathways as the $w_4^-$ ion.

In particular in the case of $w_4^-$, the evolution of the curve suggests that several ion populations exist, that decomposed through either slow or fast dissociation rate constants. In our opinion the slow dissociation rate constant population may correspond to relatively long-lived complexes (ion-dipole e.g., $[w_4^-, a_2^{\bullet}]$) that can be ejected prior to their dissociations (i.e., $[w_4^-, a_2^{\bullet}] \rightarrow w_4^- + a_2^{\bullet}$). The existence of such complexes has been considered in particular in the case of peptides and their formation allows to explain the formation of c$^{\bullet}$/z' ion pairs in addition to the conventional c/z$^{\bullet}$ ions usually observed [35]. This probably explains why the double resonance curves of $a_i^{\bullet}$ and $w_j$ ions present a similar trend. It is noteworthy that even with relatively high ejection amplitude, part of the $w_4^-$ ions remained corresponding to very fast dissociation processes. We cannot rule out that a fraction of the $w_4^-$

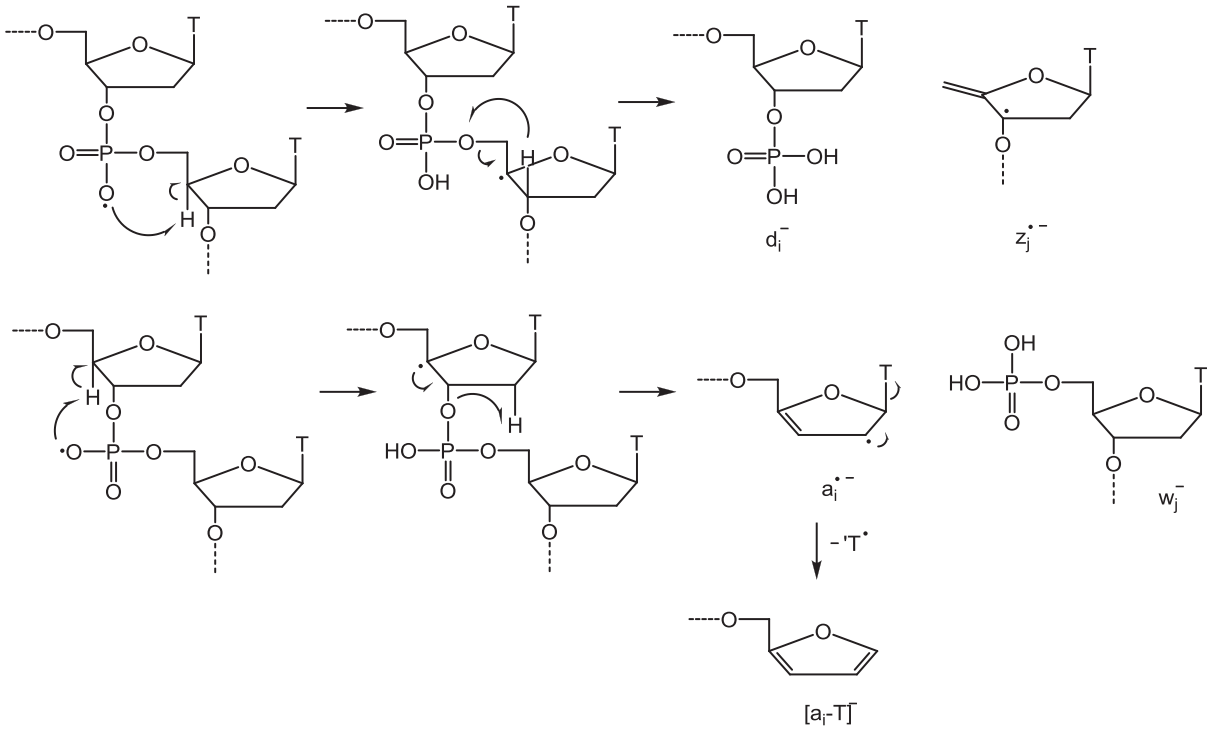

**Scheme 2.** Proposed mechanism for DNA electron detachment dissociation.

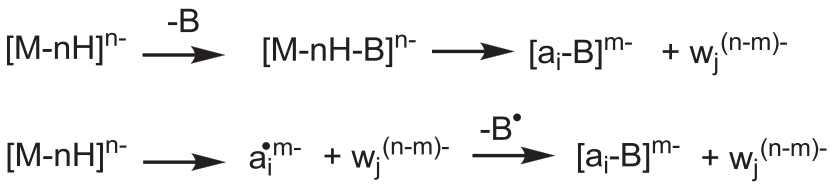

**Scheme 3.**

and $w_5^-$ ions could come from the "normal" dissociation process. In the SORI-CID spectrum of $[M-2H]^{2-}$ ion for $d(T_2AT_3)$, the $w_4^{2-}$ and $w_5^{2-}$ ions were detected. In the same way the charge reduced $[M-2H]^{\bullet-}$ ion could yield the $w_4^-$ and $w_5^-$ ion through a charge driven decomposition pathway, in this case the radical have to be localized on the neutral.

In addition, our experiments showed that thymine is the unique base lost as a radical. No loss of other nucleobase radical was observed. Hakansson and co-workers [23] performed EDD experiment with $[dA_6\text{-}2H]^{2-}$ and found the same radical ion series ($a_4^{\bullet-}/z_4^{\bullet-}$ and $a_5^{\bullet-}/z_5^{\bullet-}$) with satellite product ions corresponding to the loss of adenine. This suggests that adenine may also be lost through a radical process, but this hypothesis must be confirmed by double resonance experiments, because adenine can easily be lost by a conventional charge driven mechanism as shown above. The relative intensity of the $w_j^-$ ions displayed in the sequential EDD–EID/SORI-CID ($MS^3$) spectra of $[d(T_2AT_3)\text{-}2H]^{2-}$ and $[d(T_2CT_3)\text{-}2H]^{2-}$ increase with the $m/z$ value of the product ions. This behavior reflects the regular distribution of charge along the sequence and shows that the fragmentation in EDD pathway is mainly independent of the nucleotide sequence. Most likely, the negative charges are randomly localized on the phosphate groups. In the recent electron photodetachment work of Gabelica et al., it was shown that the electron detachment efficiency was in the order $dG_6 > dT_6 > dA_6 > dC_6$. The photodetachment effectiveness is therefore strongly base dependent [52]. In particular, guanine which has the lowest ionization energy and lower electron affinity [53,54] yielded a higher efficiency of electron photodetachment under UV irradiation at 260 nm [55]. Other studies showed that when the DNA strand contains guanine, the highest occupied molecular orbital can be located on the base and not on the phosphate [56,57].

Based on our experimental results, a mechanism is proposed for radical driven dissociation of DNA by EDD process (Scheme 2) were the charge is spectator. It is considered that the negative charge is initially on the phosphate group. Electron detachment yields an unstable radical phosphate. In Scheme 2a, a 1–5 hydrogen transfer yields a more stable tertiary radical. Consecutively, a 1–4 hydrogen transfer, leads to the formation of the complementary $z_i^\bullet$ and $d_j$ ions. Finally, loss of 'T$^\bullet$ yields the $[z_i\text{-}T]^-$ ion. In a very analogous way, Scheme 2b, allows to explain the formation of the $a_j^\bullet$, $[a_i\text{-}T]^-$ and $w_j$ ion series.

## 5. Conclusion

EDD dissociation of DNA shows abundant loss of thymine. It is favored by a radical process whereas it is very difficult to achieve with conventional dissociation processes due to its lower proton affinity. In fact, with vibrational activation modes, the loss of nucleobases is the first rupture leading to the $[a_i\text{-}B]^-$ and $w_j^-$ ion series.

Our sequential EDD/SORI-CID $MS^3$ and double resonance experiments showed that all fragment ions involving the loss of thymine in the EDD spectra come from the $a_i^\bullet$ radical ion. The combination of double resonance and EDD/SORI-CID allows decoupling of these two processes which distinguishes the fragment ions that were pro-

duced from EID and those produced from "pure" EDD. The results of EDD, EDD/SORI-CID $MS^3$ and double resonance confirm the conclusion of Kinet et al. [48] that in EDD the base loss occurs after cleavage of the sequence while with vibrational activation the base loss is the origin of the DNA backbone cleavages as summarized in Scheme 3. We presented an evolution of the ion abundances as a function of double resonance ejection amplitude in order to obtain information on the kinetics of the different dissociation processes. Two mechanisms involving radical driven pathways have been proposed concerning only the thymine base, because no loss of the other nucleobase radical was observed. Finally it was demonstrated that the "pure" EDD processes are very random along the sequence whereas some more specific cleavages are produced through EID. In comparison with vibrational activation processes the EDD technique is a complementary tool for DNA structure determination. In addition, the EDD/SORI-CID method allows obtaining a specific mode of EDD fragmentation of oligonucleotides.

## References


[1] J.B. Fenn, M. Mann, C.K. Meng, S.F. Wong, C.M. Whitehouse, Electrospray ionization for mass spectrometry of large biomolecules, Science 246 (1989) 64–71.
[2] H. Köster, K. Tang, D.-J. Fu, A. Braun, D. van den Boom, C.L. Smith, R.J. Cotter, C.R. Cantor, A strategy for rapid and efficient DNA sequencing by mass spectrometry, Nat. Biotechnol. 14 (1996) 1123–1128.
[3] R.H. Griffey, M.J. Greig, H.J. Gaus, K. Liu, D. Monteith, M. Winniman, L.L. Cummins, Characterization of oligonucleotide metabolism in vitro via liquid chomatography/electrospray in tandem mass spectrometry with a quadrupole ion trap mass spectrometer, J. Mass Spectrom. 32 (1997) 305–313.
[4] X. Guo, M.F. Bruist, D.L. Davis, C.M. Bentzley, Secondary structural characterization of oligonucleotide strands using electrospray ionization mass spectrometry, Nucleic Acids Res. 33 (2005) 3659–3666.
[5] G. Chowdhury, F.P. Guengerich, Direct detection and mapping of sites of base modification in DNA fragments by Tandem Mass Spectrometry, Angew. Chem. Int. Ed. 47 (2008) 381–384.
[6] J.W. Flora, J.C. Hannis, D.C. Muddiman, High-mass accuracy of product ions produced by SORI-CID using a dual electrospray ionization source coupled with FTICR mass spectrometry, Anal. Chem. 73 (2001) 1247–1251.
[7] K.X. Wana, M.L. Gross, Fragmentation mechanisms of oligodeoxynucleotides: effects of replacing phosphates with methylphosphonates and thymines with other bases in T-rich sequences, J. Am. Soc. Mass Spectrom. 12 (2001) 580–589.
[8] T.M. Selina Monn, S. Schürch, New aspects of the fragmentation mechanisms of unmodified and methylphosphonate-modified oligonucleotides, J. Am. Soc. Mass Spectrom. 18 (2007) 984–990.
[9] K.X. Wan, J. Gross, F. Hillenkamp, M.L. Gross, Fragmentation mechanisms of oligodeoxynucleotides studied by H/D exchange and electrospray ionization tandem mass spectrometry, J. Am. Soc. Mass Spectrom. 12 (2001) 193–205.
[10] Z. Wang, K.X. Wan, R. Ramanathan, J.S. Taylor, M.L. Gross, Structure and fragmentation mechanisms of isomeric T-rich oligodeoxynucleotides: a comparison of four tandem mass spectrometric methods, J. Am. Soc. Mass Spectrom. 9 (1998) 683–691.
[11] A.K. Vrkic, R.A.J. O'Hair, S. Foote, G.E. Reid, Fragmentation reactions of all 64 protonated trimer oligodeoxynucleotides and 16 mixed base tetramer oligodeoxynucleotides via tandem mass spectrometry in an ion trap, Int. J. Mass Spectrom. 194 (2000) 145–164.
[12] N. Russo, M. Toscano, A. Grand, F. Jolibois, Protonation of thymine, cytosine, adenine, J. Comput. Chem. 19 (1998) 989–1000.
[13] R.A. Zubarev, D.M. Horn, E.K. Fridriksson, N.L. Kelleher, N.A. Kruger, M.A. Lewis, B.K. Carpenter, F.W. McLafferty, Electron capture dissociation for structural characterization of multiply charged protein cations, Anal. Chem. 72 (2000) 563–573.
[14] R.A. Zubarev, Reactions of polypeptide ions with electrons in the gas phase, Mass Spectrom. Rev. 22 (2003) 57–77.
[15] R.A. Zubarev, Electron-capture dissociation tandem mass spectrometry, Curr. Opin. Biotechnol. 15 (2004) 12–16.
[16] J.E.P. Syka, J.J. Coon, M.J. Schroeder, J. Shabanowitz, D.F. Hunt, Peptide and protein sequence analysis by electron transfer dissociation mass spectrometry, Proc. Natl. Acad. Sci. U.S.A. 101 (2004) 9528–9533.
[17] E. Mirgorodskaya, P. Roepstorff, R.A. Zubarev, Localization of O-glycosylation sites in peptides by electron capture dissociation in a Fourier transform mass spectrometer, Anal. Chem. 71 (1999) 4431–4436.
[18] B.A. Budnik, K.F. Haselmann, R.A. Zubarev, Electron detachment dissociation of peptide di-anions: an electron–hole recombination phenomenon, Chem. Phys. Lett. 342 (2001) 299–302.
[19] J.J. Wolff, I.J. Amster, L. Chi, R.J. Linhardt, Electron detachment dissociation of glycosaminoglycan tetrasaccharides, J. Am. Soc. Mass Spectrom. 18 (2007) 234–244.
[20] Y. Xu, C. Afonso, R. Wen, J.-C. Tabet, Investigation of double-stranded DNA/drug interaction by ESI/FT ICR: orientation of dissociations relates to stabilizing salt bridges, J. Mass Spectrom. 43 (2008) 1531–1544.
[21] T.W. Bentley, R.A.W. Johnstone, Mechanism and structure in mass spectrometry: a comparison and other chemical processes, Adv. Phys. Org. Chem. 8 (1970) 151–269.
[22] R.B. Cody, B.S. Freiser, Electron impact excitation of ions from organics: an alternative to collision induced dissociation, Anal. Chem. 51 (1979) 547–551.
[23] J. Yang, J. Mo, J.T. Adamson, K. Hakansson, Characterization of oligodeoxynucleotides by electron detachment dissociation Fourier transform ion cyclotron resonance mass spectrometry, Anal. Chem. 77 (2005) 1876–1882.
[24] J. Yang, K. Hakansson, Characterization of oligonucleotide fragmentation pathways in infrared multiphoton dissociaton and electron detachment dissociation by Fourier transform ion cyclotron double resonance, J. Mass Spectrom. 15 (2009) 293–304.
[25] V. Gabelica, F. Rosu, E. De Pauw, R. Antoine, T. Tabarin, M. Broyer, P. Dugourd, Electron photodetachment dissociation of DNA anions with covalently or noncovalently bound chromophores, J. Am. Soc. Mass Spectrom. 18 (2007) 1990–2000.
[26] R. Antoine, L. Joly, T. Tabarin, M. Broyer, P. Dugourd, J. Lemoine, Photoinduced formation of radical anion peptides. Electron Photodetachment dissociation experiments, Rapid Commun. Mass Spectrom. 21 (2007) 265–268.
[27] B. Liu, P. Hvelplund, S. Brøndsted Nielsen, S. Tomita, Electron loss and dissociation in high energy collisions between multiply charged oligonucleotide anions and noble gases, Int. J. Mass Spectrom. 230 (2003) 19–24.
[28] P. Hvelplund, S.B. Nielsen, M. Sørensen, J.U. Andersen, T.J.D. Jørgensen, Electron loss from multiply protonated lysozyme ions in high energy collisions with molecular oxygen, J. Am. Soc. Mass Spectrom. 12 (2001) 889–893.
[29] A. Scott, McLuckey, G.J. Van Berkel, G.L. Glish, Tandem mass spectrometry of small, multiply charged oligonucleotides, J. Am. Soc. Mass Spectrom. 3 (1992) 60–70.
[30] H.J. Yoo, H. Liu, K. Hakansson, Infrared multiphoton dissociation and electron-induced dissociation as alternative MS/MS strategies for metabolite identification, Anal. Chem. 79 (2007) 7858–7866.
[31] M.B. Comisarow, V. Grassi, G. Parisod, Fourier transform ion cyclotron double resonance, Chem. Phys. Lett. 57 (1978) 413–416.
[32] J.C. Jurchen, D.E. Garcia, E.R. Williams, Gas-phase dissociation pathways of multiply charged peptide clusters, J. Am. Soc. Mass Spectrom. 14 (2003) 1373–1386.
[33] S. Bourgoin-Voillard, E.-L. Zins, F. Fournier, Y. Jacquot, C. Afonso, C. Pèpe, G. Leclercq, J.-C. Tabet, Stereochemical effects during $[M-H]^-$ dissociations of epimeric 11-OH-17β-estradiols and distant electronic effects of substituents at C(11) position on gas phase acidity, J. Am. Soc. Mass Spectrom. 20 (2009) 2318–2333.
[34] C.B. Theissling, N.M.M. Nibbering, S. Meyerson, The long-lived molecular ion of propionitrile: an ion cyclotron resonance study, Org. Mass Spectrom. 11 (1976) 838–843.
[35] C. Lin, J.J. Cournoyer, P.B. O'Connor, Use of a double resonance electron capture dissociation experiment to probe fragment intermediate lifetimes, J. Am. Soc. Mass Spectrom. 17 (2006) 1605–1615.
[36] R.C. Dunbar, Ion-molecule chemistry of diborane by ion cyclotron resonance, J. Am. Chem. Soc. 90 (1968) 5676–5682.
[37] M.T. Bowers, D.D. Elleman, J.L. Beauchamp, Ion cyclotron resonance of olefins. I. Study of the ion-molecule reactions in electron-impacted ethylene, J. Phys. Chem. 72 (10) (1968) 3599–3612.
[38] J.L. Beauchamp, M.C. Caserio, Ion-molecule reactions of 2-butanol by ion cyclotron resonance spectroscopy, J. Am. Chem. Soc. 94 (8) (1972) 2638–2646.
[39] B.S. Freiser, T.B. McMahon, J.L. Beauchamp, Ion ejection phenomena in ion cyclotron double resonance experiments, Int. J. Mass Spectrom. Ion Phys. 12 (3) (1973) 249–255.
[40] R. Houriet, J.-C. Tabet, Ion-molecule reactions in the gas phase. II. Bimolecular nucleophilic substitution from adduct ions of 2-cyclohexenol and ammonia studied by ion cyclotron resonance spectroscopy, Nouv. J. Chim. 6 (11) (1982) 565–569.
[41] S. Alves, A. Woods, J.-C. Tabet, Charge state effect on the zwitterion influence on stability of non-covalent interaction of single-stranded DNA with peptides, J. Mass Spectrom. 42 (2007) 1613–1622.
[42] F. Fournier, B. Remaud, T. Blasco, J.C. Tabet, Ion–dipole complex formation from deprotonated phenol fatty acid esters evidenced by using gas-phase labeling combined with tandem mass spectrometry, J. Am. Soc. Mass Spectrom. 4 (1993) 343–351.
[43] F. Fournier, M.-C. Perlat, J.-C. Tabet, Control of internal proton transfers on ion-dipole complexes from $[M-H]^-$ ions of diphenol esters, Rapid Commun. Mass Spectrom. 9 (1995) 13–17.
[44] A. Delvolve, J.-C. Tabet, S. Bregant, C. Afonso, F. Burlina, F. Fournier, Charge dependant behavior of PNA/DNA/PNA triplexes in gas phase, J. Mass Spectrom. 41 (2006) 1498–1508.
[45] M. Boutin, C. Bich, C. Afonso, F. Fournier, J.-C. Tabet, Negative-charge driven fragmentations for evidencing zwitterionic forms from doubly charged copped peptides, J. Mass Spectrom. 42 (2007) 25–35.
[46] S. Alves, A. Woods, A. Delvolve, J.-C. Tabet, Influence of salt bridge interactions on the gas-phase stability of DNA/peptide complexes, Int. J. Mass Spectrom. 43 (11) (2008) 1531–1544.
[47] E.P. Hunter, S.G. Lias, Evaluated gas phase basicities and proton affinities of molecules: an update, J. Phys. Chem. Ref. Data 27 (1998) 413–656.
[48] C. Kinet, V. Gabelica, D. Balbeur, E. De Pauw, Electron detachment dissociation (EDD) pathways in oligonucleotides, Int. J. Mass Spectrom. 283 (2009) 206–213.
[49] H. Lioe, R.A.J. O'Hair, Comparison of collision-induced dissociation and electron-induced dissociation of singly protonated aromatic amino

acids, cystine and related simple peptides using a hybrid linear ion trap–FT-ICR mass spectrometer, Anal. Bioanal. Chem. 389 (2007) 1429–1437.
[50] J.J. Wolff, T.N. Laremore, H. Aslam, R.J. Linhardt, I.J. Amster, Electron-induced dissociation of glycosaminoglycan tetrasaccharides, J. Am. Soc. Mass Spectrom. 19 (2008) 1449–1458.
[51] S. Bourgoin-Voillard, E.-L. Zins, F. Fournier, Y. Jacquot, C. Afonso, C. Pèpe, G. Leclercq, J.-C. Tabet, Stereochemical effects during $[M-H]^-$ dissociations of epimeric 11-OH-17-estradiolsand distant electronic effects of substituents at C(11) position on gas phase acidity, J. Am. Soc. Mass Spectrom. 20 (2009) 2318–2333.
[52] V. Gabelica, F. Rosu, T. Tabarin, C. Kinet, R. Antoine, M. Broyer, E. De Pauw, P. Dugourd, Base-dependent electron photodetachment from negatively charged DNA strands upon 260-nm laser irradiation, J. Am. Chem. Soc. 129 (2007) 4706–4713.
[53] E.S. Chen, E.C.M. Chen, The role of spin in biological processes: $O_2$, NO, nucleobases, nucleosides, nucleotides and Watson–Crick base pairs, Mol. Simul. 35 (2009) 719–724.
[54] D Roca-Sanjuán, M. Merchán, L. Serrano-Andrés, M. Rubio, ab initio determination of the electron affinity of DNA and RNA nucleobase, J. Phys. Chem. 129 (2008) 095104.
[55] S.D. Wetmore, R.J. Boyd, L.A. Eriksson, The IPs and EAs of the DNA bases, Chem. Phys. Lett. 322 (2000) 129–135.
[56] X. Yang, X.B. Wang, E.R. Vorpagel, L.S. Wang, Direct experimental observation of the low ionization potentials of guanine in free oligonucleotides using photoelectron spectroscopy, Proc. Natl. Acad. Sci. U.S.A. 101 (2004) 17588–17592.
[57] N.S. Kim, P.R. LeBreton, UV photoelectron and ab initio quantum mechanical evaluation of nucleotideionization potentials in water-counterion environments: pipolarization effects on DNA alkylation by carcinogenic methylating agents, J. Am. Chem. Soc. 118 (1996) 3694–3707.